THE THERMODYNAMICS OF HYDROGEN MICRO-SPHERES AS INTERNAL TARGETS IN ION STORAGE RINGS

Bertil Trostell
University of Uppsala, Department of Neutron Research
S-611 82 Nyköping, Sweden

Abstract: Solid hydrogen micro-spheres are being considered for use as internal targets at the CELSIUS electron cooled storage ring in Uppsala. The main features of the target concept are high luminosity, $\geq 10^{32}$ $cm^{-2}s^{-1}$, and a solid angle close to 4π available for detection of secondaries. Preliminary computer simulations of pellet target thermodynamics have been performed, with the purpose to obtain information on minimizing the vapor load rate at the beam intersection.

Introduction

An idea to use hydrogen micro-spheres as internal targets in the CELSIUS electron cooled ion storage ring in Uppsala [1], has lead to a proposal on developing a hydrogen pellet target facility for the purpose of light meson rare decay measurements [2]. The target generation scheme is based on the technique developed by a group at the University of Illinois at Urbana-Champaign [3] for the purpose of continuous refueling of fusion tokamak reactors by injection of hydrogen isotopes. The experimental design for rare decay studies relies on high luminosity using hydrogen target, of the order 10^{32} $cm^{-2}\cdot s^{-1}$, and close to 4π solid angle detection geometry, properties at present not known to be achievable using any other internal target concept. An additional advantage offered, is the possibility to track the spatially well defined targets by means of optical techniques for the purpose of reaction vertex determination.

A conceptual design of the hydrogen pellet target generator and collector in the proposed WASA experimental station [2] is shown in Fig. 1. A liquid hydrogen jet, having a diameter and velocity of order 10^{-5} m and 10 m/s respectively, is broken up into uniformly sized and spaced droplets at near triple point conditions by means of acoustical excitation. The droplets are allowed to develop a frozen surface shell due to evaporation before they are injected into high vacuum through a differentially pumped section. The gas flow conditions here are expected to cause an increase in velocity to about 100 m/s and the so formed partially frozen pellets are aimed to intersect the stored proton beam and finally collected in a cryogenic dump volume.

Apart from the mass present in the hydrogen pellet targets themselves, the evaporation rate from the targets is of crucial importance to the stored ion beam life time. A computer code has therefore been written, which simulates the hydrogen pellet target thermodynamics, assuming a stored proton beam. Some very preliminary results from these simulations, with specific relevance for WASA, will be presented here.

Differential Equation

The energy transport within a hydrogen micro-sphere target is governed by the parabolic differential equation

A conceptual hydrogen pellet target
and the WASA 4π detector

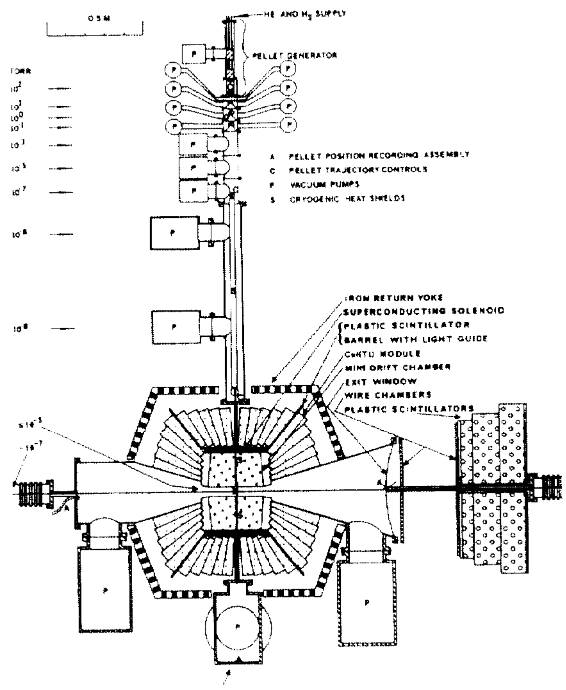

Figure 1.

$$\rho\cdot c\cdot\frac{\partial T}{\partial t}\cdot r^2=\frac{\partial}{\partial r}\left(\kappa\cdot\frac{\partial T}{\partial r}\cdot r^2\right)+\rho\cdot f\cdot S\cdot r^2,\quad 0<r<R \qquad (1)$$

where
$T(r,t)$=absolute temperature
t=time
ρ=hydrogen specific weight (82.3 $kg\cdot m^{-3}$) [4]
$c(T)$=specific heat of hydrogen [4,5]
$\kappa(T)$=thermal conductivity of hydrogen [4]
f=proton flux at the target intersection
$S(T_p)$=hydrogen stopping power for protons [6]
$R(t)$=actual radius of the hydrogen sphere

Phase transitions have to be considered at two concentric isothermal surfaces of the hydrogen sphere, the outer one where the transition to the gaseous phase takes place at a varying temperature, and an inner one where the transition between the liquid and solid phases occurs at constant temperature. In addition, the time dependence of the radii of these spherical surfaces has to be taken into account.

The boundary condition at the liquid-solid interface can be expressed as

$$\frac{\partial r}{\partial t}=\frac{1}{\rho\cdot l_f}\cdot\left\{\left[\kappa\cdot\frac{\partial T}{\partial r}\right]_s-\left[\kappa\cdot\frac{\partial T}{\partial r}\right]_l\right\},\quad T=T_{tr} \qquad (2)$$

where
l_f=latent heat of fusion ($5.804\cdot 10^4$ J/kg) [4]
T_{tr}=triple point temperature (13.96 K) [4]
and the indices s and l refer to the solid and liquid phase at the triple point temperature respectively.

Considering the energy balance at the outer surface we can write these boundary conditions as

$$\frac{\partial r}{\partial t}=\frac{1}{\rho}\cdot\varnothing,\quad r=R \tag{3}$$

$$-\kappa\cdot\frac{\partial T}{\partial r}=l_v\cdot\varnothing-P,\quad r=R \tag{4}$$

where

$\varnothing(T)$=hydrogen vapor pressure [4] dependent mass flux due to evaporation [7]

$l_v(T)$=latent heat of vaporization/sublimation of the hydrogens [4]

$P(T)$=absorbed thermal radiation flux [7]

Finally, the initial temperature distribution is given according to

$$T(r,0)=\Theta(r),\quad 0\leq r\leq R \tag{5}$$

and for symmetry reasons we also have

$$\frac{\partial T(0,t)}{\partial r}=0 \tag{6}$$

The results presented here have been obtained by solving this equation numerically using an implicit discretizing scheme [8].

Target Size Considerations

An important parameter when considering nuclear or particle physics experiments at a storage ring facility like CELSIUS is the available luminosity. In order to facilitate reaction vertex determination by optical tracking of the pellets in the proton beam, we assume that, at each instant, just one pellet is present in the ion beam. The available experimental luminosity, using a hydrogen pellet target, is then given by

$$L=\frac{2\cdot M\cdot f}{m_H} \tag{7}$$

M=actual mass of the pellet

m_H=molecular mass (3.3472·10-27 kg) [4]

In the following, the design luminosity for π^0 rare decay measurements, 10^{32} $cm^{-2}\cdot s^{-1}$, using the proposed WASA experimental station, will be considered as typical in the simulations. π^0 mesons will in this case be produced using the $pp\rightarrow pp\pi^0$ reaction at T_p=550 MeV [2] thereby taking advantage of the maximum electron velocity available for cooling at CELSIUS [9] in order to obtain a high π^0 production cross section. With

O=storage ring circumference (81.8 m) [9]

r_b=proton beam radius ($1.5\cdot10^{-3}$ m) [2]

n_p=number of stored protons (10^{10}) [2]

yielding

$f=4\cdot10^{21}$ $m^{-2}\cdot s^{-1}$

targets with diameters of 10, 21 and 46 μm will be needed to reach luminosities of 10^{31}, 10^{32} and 10^{33} $cm^{-2}\cdot s^{-1}$ respectively.

Target Generation

The targets are initially generated as micro-spheres in the liquid phase at triple point conditions, with a frozen surface shell developed before the injection into vacuum, as was briefly described in the introduction. It is therefore reasonable to give the initial temperature distribution (5) according to

$$T(r,0)=T_{tr},\quad 0\leq r\leq R \tag{8}$$

where a thin surface shell is solid. The pellet velocities of ≈ 100 m/s, acquired during the injection into high vacuum, determine the time available for cooling the micro-spheres before entering the proton beam to a few tens of a millisecond, since the extension of the target generating structure for practical reasons is limited to typically a few meters.

The time dependence of the surface temperatures of cooling hydrogen micro-spheres are shown in Fig. 2. Heat radiation shields, having temperatures of 300, 77 and 4 K respectively, are assumed to surround the targets in flight. As can be seen, the surface temperatures approach equilibrium values, depending on the radiated thermal heat flux, where the energy flux due to evaporation is balanced. The temperature distributions within the pellets become isotropic after roughly 10^{-4} s except for the largest one, which then still has a mixed phase composition and a full ms is needed. The relative mass losses during a second of cooling is 15 % except for the case of room temperature heat shield, where most of the pellet evaporates. The smallest one will not even survive. Typical mass losses after 30 ms of cooling are in the range 15 - 20 % in all cases.

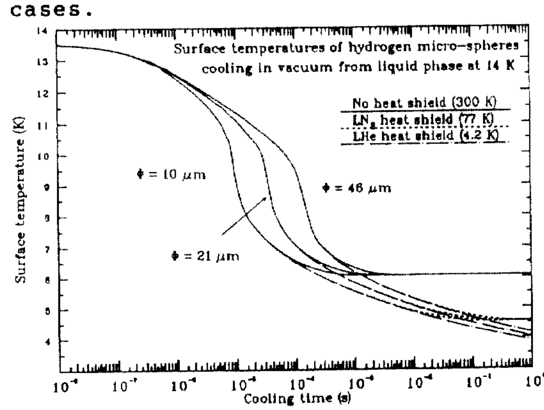

Figure 2.

Since the narrow tube in the mini drift chamber of WASA, through which the targets enter the beam intersection area, has a length of 0.2 m, we consider the gas load rate from pellets within this range entering into the beam tube and disregard influences from greater distances. Thus, the instant evaporation rate of one pellet (see Fig. 3), determined by the surface temperature after 30 ms of cooling and the surface area, should be multiplied by 70 in order to obtain this contribution to the total gas load rate. The results are shown in Table I.

TABLE I.

Contribution to the total gas load rate from 70 targets approaching the beam ($Pa\cdot m^3\cdot s^{-1}$)

Diameter (μm)	Heat shield temperature (K) 4	77	300
10	$6.4\cdot10^{-8}$	$9.8\cdot10^{-8}$	$1.2\cdot10^{-5}$
21	$6.7\cdot10^{-7}$	$8.2\cdot10^{-7}$	$5.7\cdot10^{-5}$
46	$7.3\cdot10^{-6}$	$7.9\cdot10^{-6}$	$2.7\cdot10^{-4}$

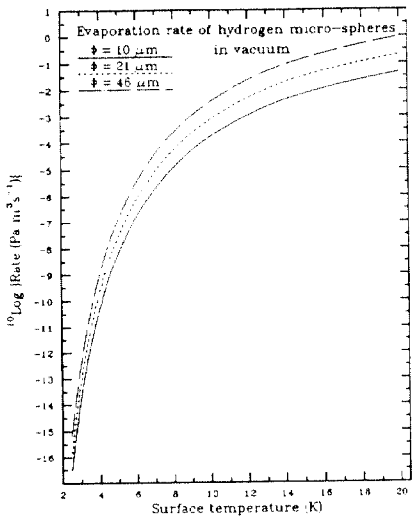

Figure 3.

Target-Proton Beam Interactions

With initial surface temperatures according to Fig. 2, the effects on surface temperature of the dwelling time in the proton beam are shown in Fig. 4. The surface temperatures again approach equilibrium values, now being dependent on size, since the power dissipated by the proton beam in the targets is a mass effect whereas the balancing evaporation is a surface effect. On larger time scales these temperatures will of course decrease as evaporation reduces the pellet masses.

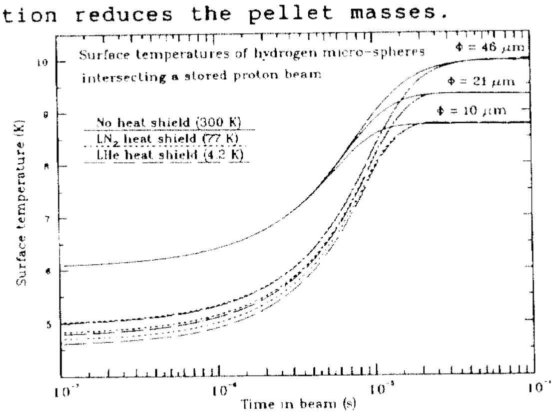

Figure 4.

The targets will traverse the proton beam in 30 μs, by coincidence being the approximate time needed to reach the equilibrium temeperatures. The initial temperature differences, when entering the beam, consequently have barely any impact on this time scale. The integrated gas load rate contribution from the one pellet in the beam is according to Table II.

TABLE II.

Contribution to the total gas load rate from the one target in the beam (Pa$\cdot$m$^3\cdot$s^{-1})

Diameter (μm)	Heat shield temperature (K) 4	77	300
10	$2.2\cdot10^{-5}$	$2.2\cdot10^{-5}$	$2.4\cdot10^{-5}$
21	$1.9\cdot10^{-4}$	$1.9\cdot10^{-4}$	$2.2\cdot10^{-4}$
46	$1.4\cdot10^{-3}$	$1.4\cdot10^{-3}$	$1.7\cdot10^{-3}$

Target Dumping

Similar to above, we consider the integrated gas load rate from the 70 pellets within 0.2 m from the beam intersection and disregard influences on the beam tube vacuum from greater distances. The results are shown in Table III. The final storage of the used targets will be made in a cryogenic dump connected to vacuum pumps.

TABLE III.

Contribution to the total gas load rate from 70 targets receding from the beam (Pa$\cdot$m$^3\cdot$s^{-1})

Diameter (μm)	Heat shield temperature (K) 4	77	300
10	$1.3\cdot10^{-5}$	$1.3\cdot10^{-5}$	$2.0\cdot10^{-5}$
21	$1.5\cdot10^{-4}$	$1.5\cdot10^{-4}$	$1.8\cdot10^{-4}$
46	$1.9\cdot10^{-3}$	$1.9\cdot10^{-3}$	$2.1\cdot10^{-3}$

Conclusions

Table IV shows the sums of the three contributions to the hydrogen vapor load rate. The different heat shields surrounding the pellets in flight have no significant impact on the gas load rate in the beam tube.

TABLE IV.

Total gas load rate from 140 hydrogen targets at the proton beam intersection (Pa$\cdot$m$^3\cdot$s^{-1})

Diameter (μm)	Heat shield temperature (K) 4	77	300
10	$3.5\cdot10^{-5}$	$3.5\cdot10^{-5}$	$5.6\cdot10^{-5}$
21	$3.4\cdot10^{-4}$	$3.4\cdot10^{-4}$	$4.6\cdot10^{-4}$
46	$3.3\cdot10^{-3}$	$3.3\cdot10^{-3}$	$4.1\cdot10^{-3}$

The conductance of the beam transport tube inside the mini drift chamber, being ≈ 0.4 m$^3\cdot$s^{-1} for hydrogen (pumping on both sides), will determine the rate at which the vapor load from the evaporating targets can be removed. If we assume that an infinite pumping speed is available outside this region, a typical vacuum in the beam tube enclosed by the mini drift chamber of $\approx 10^{-3}$ Pa should thus be obtainable at the design luminosity of WASA according to Table IV. This corresponds to a stray event rate being a few times 10^{-3} of the event rate from the target itself. The largest target size may cause too severe deterioration of the storage ring vacuum to be acceptable.

References

[1] S. Kullander, Proc. AIP Conf. 128, 1985
[2] Wide Angle Shower Apparatus, Proposal for a Detector at CELSIUS from the WASA Collaboration, Uppsala, Sweden, 1987
[3] C.A. Foster, K. Kim, R.J. Turnbull and C.D. Hendricks, "Apparatus for Producing Uniform Solid Spheres of Hydrogen," Rev. Sci. Instrum., vol. 48, pp.625, 1977
[4] P.C. Souers, "Cryogenic Hydrogen Data Pertinent to Magnetic Fusion Energy," Report UCRL-52628, 1979
[5] P.C. Souers and R.T. Tsugawa, "Estimated Heat Capacity, Enthalpy, Thermal Conductivity and Diffusivity of Solid D-T," Report UCRL-52068, 1976
[6] H.H. Andersen and J.F. Ziegler, Hydrogen Stopping Power and Ranges in All Elements. Pergamon Press, 1977
[7] F. Reif, Fundamentals of Statistical and Thermal Physics. McGraw-Hill, 1965
[8] S.E. Koonin, Computational Physics. Menlo Park: Benjamin/Cummings, 1986
[9] S. Holm, A. Johansson, S. Kullander and D Reistad, "New Accelerators in Uppsala," Physica Scripta, vol. 34, pp.513, 1986